



# THERMAL PERFORMANCE OF LOW-COST COOLING SYSTEMS FOR TRANSMIT/RECEIVE MODULES OF PHASED ARRAY ANTENNAS WITH AND WITHOUT GRAVITY HEAT PIPES

Yu.E. Nikolaenko<sup>a</sup>, D.V. Pekur<sup>b\*</sup>, V.Yu. Kravets<sup>a</sup>, V.M. Sorokin<sup>b</sup>, D.V. Kozak<sup>a</sup>, R.S. Melnyk<sup>a</sup>, L.V. Lipnitskiy<sup>a</sup>,  
A.S. Solomakha<sup>a</sup>

<sup>a</sup> National Technical University of Ukraine "Igor Sikorsky Kyiv Polytechnic Institute", Heat-and-Power Engineering Department, Kyiv, Ukraine

<sup>b</sup> V. Lashkaryov Institute of Semiconductor Physics, National Academy of Sciences of Ukraine, Department of Optoelectronics, Kyiv, Ukraine

## ABSTRACT

This study compares thermal characteristics of two design versions of a new low-cost air-cooling system with a standard heat sink profile and built-in flat heat pipes of a simple design with a similar cooling system design without the heat pipes. The aim of the work is to determine the thermal characteristics and choosing the most effective option in a practical context. Using computer simulation in the Solidworks Flow Simulation standard software package allowed determining how the temperature of 8 transistors with a total power of 224 W was affected by changes in air velocity from 1 to 30 m/s, effective thermal conductivity from 1 to 30 kW/(m<sup>2</sup>·°C), and the number of heat pipes from 8 to 16 pieces. It was determined that the maximum temperature decrease for the transistors is observed in the velocity range from 1 to 10 m/s for all the studied cooling system designs. Using 8 HPs with effective thermal conductivity of 5 kW/(m<sup>2</sup>·°C) allowed lowering the maximum temperature value on the mounting surface by 22.56°C (from 85.03 to 62.47°C) and reducing surface temperature unevenness more than twice – from 55.7 to 25.93°C). Increasing the effective thermal conductivity of the heat pipes from 1 to 10 kW/(m<sup>2</sup>·°C) reduced the temperature of the hottest transistor by 15 – 20°C, depending on the system design version. Further increase of the effective thermal conductivity to 30 kW/(m<sup>2</sup>·°C) reduced the temperature by only 1 – 2°C. Doubling the number of the heat pipes from 8 to 16 did not significantly improve the thermal characteristics of the transistors (by 3.3 – 2.8°C). When the air velocity was increased from 1 to 10 m/s, the total thermal resistance decreased most significantly for the cooling system with 8 heat pipes, namely from 0.179 to 0.068°C/W, while for the version with 16 heat pipes it decreased from 0.164 to 0.054°C/W. Thus, the cooling system with 8 heat pipes with an effective thermal conductivity of up to 10 kW/(m<sup>2</sup>·°C) and an air velocity in the heat sink channels from 1 to 10 m/s proves to be best suited for practical use in T/R modules.

**Keywords:** Transmit/receive module; low-cost air cooling system; thermal characteristics; heat sink; gravity heat pipe

## 1. INTRODUCTION

Modern radar systems are based on the highly efficient active phased antenna arrays (APAA) technology (Jarndal, 2007; Shinohara, 2013). APAAs must be able to provide a certain level of output power of the emitted signal and remain functional under toughest operating environments, such as high ambient temperatures. APAA development trends were set out in the following studies: Park, J.S. *et al.*, 2021; Park, T.-Y. *et al.*, 2021; Carlson *et al.*, 2017; Aslan *et al.*, 2018. Modern APAA contain up to tens of thousands of transmit/receive (T/R) modules (Haupt and Rahmat-Samii, 2015) and are excessively expensive, about \$1 million per square meter (Barbettey, 2011). Over the recent decades, much attention has been given to reducing the cost of APAAs by improving the circuitry, using new materials, increasing integration density of microchips, and improving both the layout of T/R modules and the technology of electrical connections (Rao *et al.*, 1996; Rebeiz *et al.*, 2017; Goel and Vinoy, 2011). The price of APAAs is also significantly affected by the cost of cooling system design (Sarcione and Puzella, 2010), but among the known publications there are virtually no studies about reducing the cost of the design of APAA cooling systems. This study aims to partially solve this problem.

During designing APAAs, the main limiting factors are their mass, size, and cost. Typically, APAAs have a complex structure and a dense arrangement of electronic components (Kopp *et al.*, 2001). This is a reason, why developing an APAA, thermal management of the electronic components requires particular attention. The most heat-loaded APAA units are transmit/receive (T/R) modules.

T/R modules are key discrete elements in APAAs and are mounted directly behind the emitter on the antenna sheet. Modern APAAs can include several tens of thousands of T/R modules (Haupt and Rahmat-Samii, 2015), each of them contains at least one output power amplifier. Depending on the frequency range in which the T/R module operates, the output power amplifiers may include transistors and microwave monolithic integrated circuits (MMIC) of various frequency bands as active devices (Rathod *et al.*, 2018; Herd and Conway, 2016; Pengelly *et al.*, 2012, Choi *et al.*, 2009). The characteristics of these elements determine the functionality and performance of the module completely. The limited conversion efficiency of the active microwave elements, however, leads to quite significant heat loads. The temperature conditions largely affect the functional characteristics, reliability and efficiency of microwave transistors and MMICs of output amplifiers, and hence the T/R module of the APAA completely (Hosseinizadeh *et al.*, 2011; Wang *et al.*, 2016).

\* Corresponding author. Email: demid.pekur@gmail.com

Thus, thermal management of the active microwave elements of the output power amplifiers of the T/R module poses a pressing issue and requires developing highly efficient cooling systems (Parlak and Yaban, 2015).

To address this issue (Parlak and Yaban, 2015; Wang *et al.*, 2016; Nikolaenko *et al.*, 2020), proposed different types of liquid cooling systems. Despite the high efficiency and diversity of liquid cooling systems, they have such common disadvantages as complexity, high cost, risk of leakages in liquid line connections, high energy consumption, etc. In study Park J.S. *et al.*, 2021, computational fluid analysis was performed by changing the number of T/R modules and the coolant mass flow rate to evaluate the cooling performance of the AESA radar coolant channel. This study established basic data on coolant operating conditions and array for designing the cooling system for an AESA radar of 1000 channels or more. Study Liang *et al.*, 2021, integrated a fluid circulation-type cold plate and array radar T/R Module to develop an integrated heat dissipation system that was suitable for high-power radar equipment.

Forced air cooling systems for T/R modules are simpler, more reliable and cheaper for manufacturing and operating (Swadish and Sangram, 2017; Maguire *et al.*, 2004; Scott and Sampson, 2003; Nikolaenko *et al.*, 2019).

Swadish and Sangram (2017) simulated the air cooling of T/R modules for the APAA consisting of 8 identical circuit boards, each containing 16 T/R modules and a unit controller. The power of one circuit board was 280 W (16 T/R modules with a power of 14 W each and a controller with a power of 56 W). The circuit boards with T/R modules and the controller were cooled by a forced air flow with an inlet air temperature of 23°C using a chiller. Such cooling system allowed keeping the maximum temperature of the T/R modules below 60°C.

Maguire *et al.* (2004) investigated the thermal conditions in a high-power radio frequency signal amplifier with an air cooling system based on an aluminum heat sink with a complex fin profile and with two 6 mm thick copper heat spreaders built into the base of the heat sink. The experimental results showed that the heat sink with copper plates has a higher efficiency compared to the heat sink without the plates. The copper plates allowed reducing the temperature of the heat sink by 4.7°C.

Qian *et al.* (2022) optimized the air-cooling heat sink for the transmitting antenna and showed that, compared with the original heat sink design, the optimized heat sink can greatly improve heat dissipation and reduce the maximum temperature of the active electronic component heat flux simulators by 8°C.

Scott and Sampson (2003) proposed an APAA air cooling system with a refrigeration machine. The cooled air is directed to the hottest electronic components, thus ensuring a required temperature of the elements. However, adding a refrigeration machine increases the mass and size of the APAA, as well as its power consumption.

The authors of (Nikolaenko *et al.*, 2019) used computer simulation to assess the efficiency of the forced air cooling system for T/R modules with a capacity of 224 W without the refrigeration machine. The research showed that when the air flow rate in the cooling channels did not exceed 6 m/s and the inlet air temperature of 40°C, the temperature near the hottest transistor was 77.1°C, and the temperature of the semiconductor crystal reached 164.1°C, which significantly exceeded the maximum allowable crystal temperature. In these researches proposed to increase the efficiency of forced air cooling of T/R modules by integrating flat heat pipes (HP) into the base of the heat sink. The HPs helped distribute local heat fluxes from high-power transistors to a larger heat-transfer surface, thus making it possible to reduce the temperature of the hottest transistors by 20.3°C.

Other known designs of HP-based cooling systems for T/R modules (Patent of Ukraine no. 139015, 2019; Xu and Qian, 2020) primarily use heat pipes with powder or metal-fiber capillary structures (Faghri, 2014; Mochizuki *et al.*, 2011; Velardo *et al.*, 2021). Such heat pipes are operational under conditions of gravity even at unfavorable orientations, when the evaporator is positioned at the same level as the condenser or

above it. This is an undeniable advantage over the HPs with other capillary structure types, such as grooved wick. A significant disadvantages of such HPs are the power-intensive, high-temperature and lengthy sintering process required to produce the capillary structure (Velardo *et al.*, 2021), which make the heat pipes themselves and the whole cooling system more expensive.

The second significant factor affecting the cost of the known designs (Nikolaenko *et al.*, 2019; Patent of Ukraine no. 139015, 2019) of air cooling systems for T/R modules is that the heat sink housing used in mentioned designs is machined from a solid aluminum billet. This manufacturing method does have certain advantages. For example, it allows producing very complex structural elements in the housing of the T/R module, including various types of cooling fins on the back of the mounting surface. However, major disadvantages of this method are a significant material waste, an expensive and time-consuming manufacturing process. The most technologically and economically feasible way of manufacturing the heat-transfer surface for the cooling system is to use a cheaper mass-produced heat sink profile in the T/R module design.

Many studies have been conducted on the use of heat pipes in cooling systems. Guo *et al.* (2020) investigated loop heat pipes. Koito (Koito, 2019a; Koito, 2019b; Koito, 2021) studied the characteristics of ultra-thin flat heat pipes. Flat heat pipes of the vapor chamber type were investigated by Mochizuki and Nguyen (2019). Sobhan and Peterson (2019) proposed a new design of a micro heat pipe array. The most attractive aspect of this design is its ease of fabrication by sandwiching an array of wires between two metal plates. Bhagata and Deshmukh, (2021); Schily and Polifke (2021) performed simulations of pulse heat pipes, which do not have a wick and are simpler and cheaper than wick heat pipes. Singh *et al.* (2019); Abdalla *et al.* (2022) investigated the possibility of using heat pipes to reduce energy consumption in data centers and air conditioning systems.

In order to reduce the cost of air cooling systems with heat sink housings and integrated heat pipes for T/R modules, this research uses computer simulation to perform the first-ever evaluation of thermal performance of the new cooling system for high-power transistors of output power amplifiers of the APAA T/R module (Patent of Ukraine no. 147733, 2021) sing lower-cost heat-transfer surfaces and heat pipes. What sets this research aside from others is that the heat-transfer surface of the heat sink housing is made of a lower-cost mass-produced heat sink profile enhanced by lower-cost flat gravity heat pipes with a threaded capillary structure (Patent of Ukraine no. 130237, 2018, Pekur, 2021) integrated into the base of the heat sink. The manufacturing technology for such heat pipes is simple and practical (Patent of Ukraine no. 133241, 2019). Operability of the pipes is achieved by positioning them inside the housing at a certain angle to the lower horizontal edge of the heat sink base, which ensures that the condenser of the HP is elevated over the evaporator in the working, tilted to the horizon, position of the APAA.

## 2. DESIGN ASPECTS OF THE NEW COOLING SYSTEM BASED ON FLAT GRAVITY HEAT PIPES

The object of computer simulation was the new promising design of air cooling system for T/R modules with a relatively cheap mass-produced heat sink profile and relatively cheap flat gravity heat pipes with a threaded capillary structure (see Fig. 1).

This cooling system design can be used for thermal management of high-power microwave transistors or MMICs of multi-channel T/R modules for APAA. The overall dimensions of the T/R module and the layout of the active heat-generating elements apply to modern T/R module designs and can be mounted in the APAA air channel, where the cooling air flow is moved by forced convection.

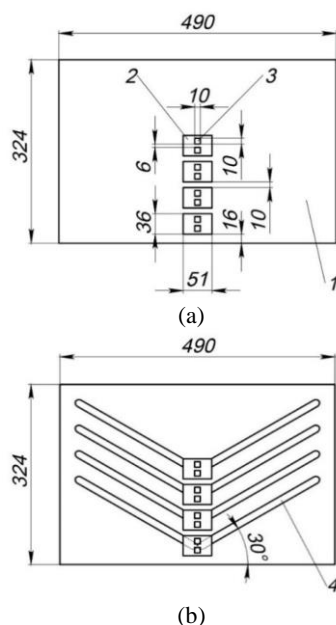


**Fig. 1** Schematic showing the mounting surface of the heat sink base of the T/R module and the arrangement of heat-generating transistors (a) and flat gravity HPs with a threaded capillary structure (b). 1 – heat sink housing base; 2 – copper mounting plate; 3 – transistor; 4 – gravity heat pipe.

## 2.1 Mounting surface of the heat sink housing base of the T/R module

The design of the mounting surface of the T/R module housing base with active microwave elements is shown in Fig. 1, and the geometric parameters of the cooling system are shown in Table 1.

The T/R module and its cooling system are so designed that the high-power active microwave semiconductor electronic components (transistors) are mounted on copper mounting plates – 2 transistors on each of the 4 plates. The size of the contact area between a copper plate and the mounting surface of the heat sink housing is 36×51 mm. The thickness of each plate is 5 mm. The plates are arranged on the mounting surface vertically along the center line of the base length. The distance between the centers of the copper plates is 46 mm, and between the lower edge of the heat sink and the bottommost copper plate – 16 mm (Fig. 1, a). The total power of all 8 transistors being 224 W, the heat flux density in the zone of thermal contact between each transistor and the copper mounting plate is 28 W/cm<sup>2</sup>.

**Table 1** Technical specifications of the new cooling system design for the T/R module.

Parameter	Value
Overall dimensions of mounting surface of heat sink housing base, mm	324×490
Dimensions of contact zones of transistors in output power amplifiers, mm	10×10
Total number of transistors in output power amplifiers	8
Dimensions of copper mounting plate, mm	51×36×5
Number of copper mounting plates, pcs.	4
Power of each transistor, W	28
Total power input to heat sink housing base, W	224

Channels of rectangular cross section (3 mm deep, 16 mm wide, 250 mm long) are machined into the heat sink base, at a 30° angle to its leading edge, on both sides of the vertical axis along which the copper plates with heat-generating transistors are mounted. The flat HPs with a threaded capillary structure in the evaporator are placed inside these

channels in reliable thermal contact to their surface. The HP evaporator sections are in thermal contact with both the aluminum heat sink housing and the copper mounting plates with transistors. The condenser sections of the HPs are located in the rectangular cross-sectional channels in the heat sink base at a certain angle along the heat sink (Fig. 1, b). When in working position, the APAA sheet is tilted at an angle to the horizon, and the condenser sections of the heat pipes take position above the evaporator sections, which makes it easier for gravity to return the condensate from the condenser to the evaporator.

## 2.2 Heat-transfer surface of the cooling system

The heat-transfer surface is the finned heat sink on the back of the mounting surface. The heat sink profile of the required width is not, however, widely available. As an alternative, it was proposed to weld two separate parts into a single heat-transfer surface. At the same time, these separate parts were made of the fragments of less expensive mass-produced heat sink profile of the required size (Fig. 2). The profile is made of aluminum-magnesium alloy AD31T5 (alloy 6063 according to EN 573-3-2009). The geometric parameters of the heat-transfer surface are shown in Table 2.

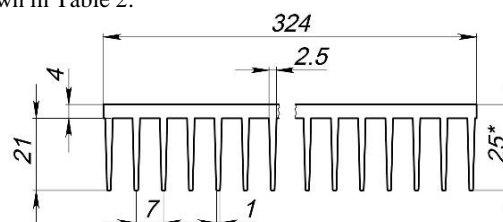


**Fig. 2** Cross-section of the welded heat-transfer surface.

The heat from the local high-power active microwave elements used in the design of the T/R module is removed via contact thermal conductivity between the transistors and copper mounting plates, via conduction through the copper plates, and via contact thermal conductivity between the copper plates and outer walls of the HPs. From the outer walls of the HPs the heat is transferred via conduction to the inner walls and further to the working fluid in the evaporation section of the HPs. Inside the operating HP, the heat is transferred from the evaporator to the condenser with minimal thermal resistance due to the closed evaporation-condensation cycle. Taking into account the operating conditions of the T/R module, the HP may be filled with ethanol, n-pentane, acetone, freon 141b, etc. From the heated outer surface of the HP the heat is transferred via contact thermal conductivity to the heat sink housing and from there along the heat sink body to the heat-transfer surface and further to the air in the cooling channels of the heat sink.

**Table 2** Geometric parameters of the heat sink profile and heat-transfer surface.

Parameter	Value
Dimensions of cross-section of heat sink profile, mm	200×25
Dimensions of cross-section of heat-transfer surface, mm	324×25
Base thickness, mm	4
Fin height, mm	21
Distance between fins, mm	7
Fins thickness at the base, mm	2.5
Fins thickness at the top, mm	1
Number of fins, pcs.	46
Number of interfin channels, pcs.	45
Cross-sectional area of 1 cooling channel ×10 <sup>-4</sup> , m <sup>2</sup>	1.1
Cross-sectional area of all cooling channels ×10 <sup>-4</sup> , m <sup>2</sup>	49.6
Area of heat-transfer surface for 0.49 m long heat sink, m <sup>2</sup>	1.090
Amount of material used ×10 <sup>-3</sup> , m <sup>3</sup>	1.463
Weight of heat sink, kg	3.951

Considering that it is a complicated and complex task to produce a physical model of the cooling system for T/R modules. The computer using the Solidworks Flow Simulation software package was performed to determine the thermal characteristics of the proposed new T/R module cooling system and to clarify the nature of the impact of effective thermal conductivity in heat pipes and air velocity in the cooling channels on the temperature of the transistors. Computer simulation has been increasingly used over the recent years to analyze the thermal regimes of heat-loaded devices and cooling systems (Koito, 2021; Zhang *et al.*, 2021; Pekur, 2020a; Pekur, 2020b).

### 3. COMPUTER SIMULATION OF THE COOLING SYSTEM FOR T/R MODULES

#### 3.1 Computer simulation technique

Simulation was performed using the Solidworks Flow Simulation standard software package. The computer simulation was performed on the air cooling system for T/R modules, which included a heat sink housing, 4 copper mounting plates, 8 heat sources, and 8 (first design option) or 16 (second design option) flat heat pipes integrated into the heat sink housing.

Using the above geometric specifications, a computer model of the cooling system was created with the Solidworks software package, and the Solidworks Flow Simulation tool was used to perform numerical simulation of the temperature distribution in the cooling system at a thermal power of 224 W (for the 8 transistors) for discrete system parameters.

The Solidworks software package was chosen for this task, because the Flow Simulation tool is fully integrated into the SolidWorks interface, which allows simulating the geometry and performing all calculations in one program. SolidWorks also makes it possible to arbitrarily select arrays of simulation results of various properties to be exported in numerical form, which allows the researcher analyze the results in numerical form or as graphs. In SolidWorks Flow Simulation, the set of problems related to heat transfer is solved using a Navier–Stokes system of equations for energy and continuity, which describe the laws of mass, momentum and energy conservation for this fluid in a nonstationary setting. Also there are used are the equations of state of the liquid components, as well as the empirical dependences of viscosity and thermal conductivity of these components on temperature, which are rather complex for analytical use.

The main stages of developing a computer model of the cooling system in SolidWorks Flow Simulation were: a) creation of a 3D model; b) imposition of simulation conditions (choosing properties for the environment and materials used in the model, setting the heat load and the area, detailing the simulation); c) simulation per se; d) visualization of the temperature fields of the elements and air, air velocities, etc.

The developed three-dimensional model of the cooling system allows calculating the thermophysical characteristics of the flows and determining the temperature fields of the surfaces of the heat sink housing.

To link the mathematical model to a specific physical problem and to the area of space in which it is solved (the so-called computational domain), it is necessary to specify the boundary conditions that will be used in the simulation.

#### 3.2 Initial and boundary conditions

The general simulation conditions for the chosen cooling system design are: heat radiation is neglected; environment – air; inlet air temperature +20 °C, atmospheric pressure 101.325 kPa.

The computational domain of the developed computer models is 490×324×31 mm (Fig. 3).

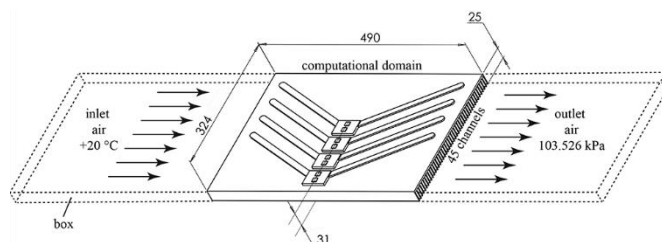


Fig. 3 Schematic representation of the calculation domain

The problem was solved in a stationary setting in keeping the requirement for the solutions to be independent from the discreteness of the computational grid. The computational domain boundaries were taken to be adiabatic.

The following assumptions were also used in the simulation:

- The effects of thermal radiation and free convection from thermally insulated surfaces were neglected.
- The simulation was performed for stationary heat exchange and air flow in the heat sink channels.
- The heat pipe was modeled as a flattened solid rod made of a material with a constant thermal conductivity equal to the chosen effective thermal conductivity of the heat pipe.
- Transistors, as heat sources, were modeled as areas with a heat flux evenly distributed over the surface.
- The thermal resistance between the elements of the cooling system (heat pipe and heat sink, heat pipe and copper plates (pallets), pallets and transistors) was assumed to be zero. The contact thermal resistance largely depends on the quality of the contacting surfaces and the medium that fills the gaps in the contact zone. This is why, when using high-quality contact surfaces of the elements and highly thermal conductive paste, our practical experience suggests that the total increase in the temperature of transistors due to contact zones does not exceed 3-4%, which is close to the modeling error.

The simulation was performed for three design options of the cooling system: 1) no HPs in the heat sink housing; 2) 8 HPs in the heat sink housing (2 HPs for each copper mounting plate); 3) 16 HPs in the heat sink housing (4 HPs for each copper mounting plate). The cooling system was simulated with the chosen design parameters of the heat-transfer surface for the air velocities in the cooling channels initially set in the range of 1 to 10 m/s (with an interval of 1 m/s), as well as for 15, 20, 25 and 30 m/s.

Other aspects taken into account during the simulation were the materials of the mounting plates (M1 copper with a thermal conductivity of 406 W/(m·°C) (Kalinchak *et al.*, 2012) and the heat sink (aluminum-magnesium alloy AD31T5 with a thermal conductivity of 183 W/(m·°C) (Beletskiy and Krivov, 2005)). Based on previous studies, the effective thermal conductivity of heat pipes was taken to be 5000 W/(m·°C) (Nikolaenko *et al.*, 2021).

In order to study how effective thermal conductivity of HPs impacts the temperature of the transistors in the T/R module, the simulation included the HPs with different values of effective thermal conductivity – in the range from 1000 to 10,000 W/(m·°C) with an interval of 1000 W/(m·°C) and in the range from 15,000 to 30,000 W/(m·°C) with an interval of 5000 W/(m·°C). To evaluate how effective the HPs are in this design, also simulated was a version of the cooling system with copper rods of the same size as the HPs with a thermal conductivity of 400 W/(m·°C).

#### 3.3 Computational grid

The simulation involves discretizing the elements of the solid body of the model and the gaseous medium of the computational domain using nonuniform computational grids. Nonuniform computational grids allow presenting a physical and mathematical description of the processes occurring in the cooling system. These processes are based on the



numerical solution of the Reynolds-averaged Navier–Stokes equations closed by the  $k-\epsilon$  turbulence model with nonequilibrium wall functions.

Computer models with a total number of elements from 2.3 to 3.2 million were used for the chosen designs of cooling systems, the dimensions of the smallest element being  $0.25 \times 0.25 \times 0.25$  mm.

The discreteness of the model's grid and its individual elements was determined automatically, depending on the complexity of their shape and geometry. The grid near the transistors, heat pipes, and the fin surface was mostly made denser than the rest of the geometry due to the large amount of fine detail and more complex geometry (see Fig. 4). The grid elements had a cubic shape with a cube side length reduced by a factor of two on each level of grid compaction. The total number of the elements used in the models is given in Table 3.

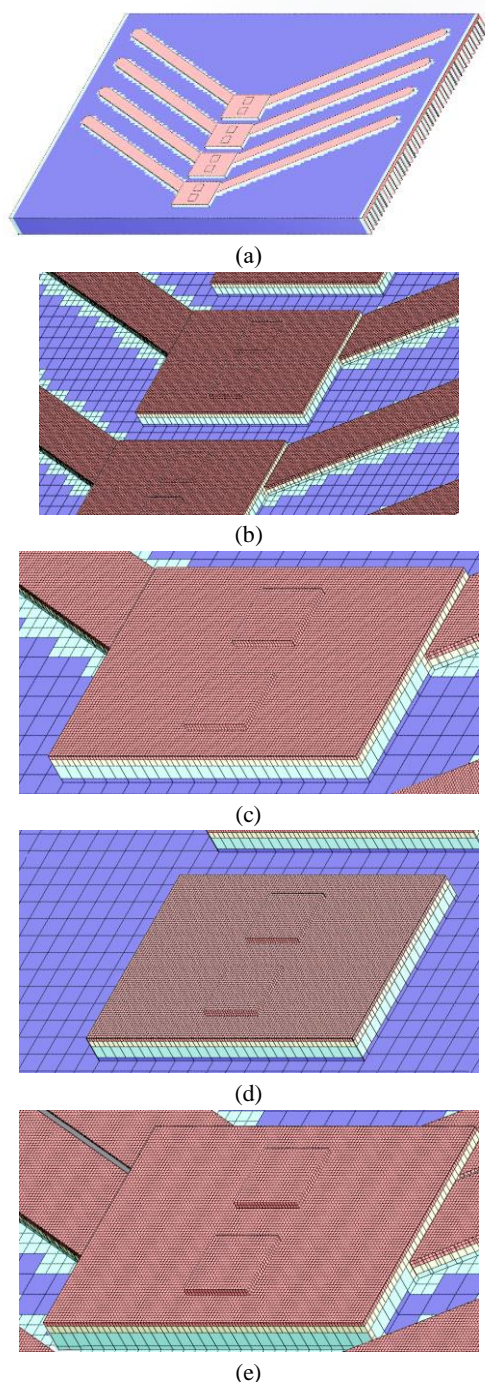


**Fig. 4** Calculation grid for solid model elements: with two HPs (a-c), without HPs (d), and with four HPs (e) for each copper mounting plate.

**Table 3** Number of elements of computational grids for cooling system models.

Parameters of elements	Number of elements		
	No HPs	With 8 HPs	With 16 HPs
Total number of elements	2 342 635	2 697 277	3 176 989
Elements in mobile medium	894 037	931 258	1 603 428
Elements in solid body	865 470	1 153 671	1 573 561
Elements at the interface between solid and gaseous mediums	583 128	612 347	954 271

To control discretization and convergence errors were used computational grids with varying degree of detail (up to 3.2 million elements). The maximum temperature of the transistor at different air velocities was chosen as a control parameter. For different discretization degrees, the error was estimated to be below 4% of the weighted average, which indicated the convergence of the results and the reliability of the computer models.

Fig. 5 shows an example of the convergence for computational grids with a discretization degree from 0.04 to 3.2 million elements with a sequential increase in the grid discretization level by a factor of 2 and an air velocity of 1 m/s. Given the complexity of the models, the number of elements was chosen as shown in Table 3. At the same time, the predicted subsequent doubling of the grid elements leads to only a slight increase in accuracy (less than 1%).

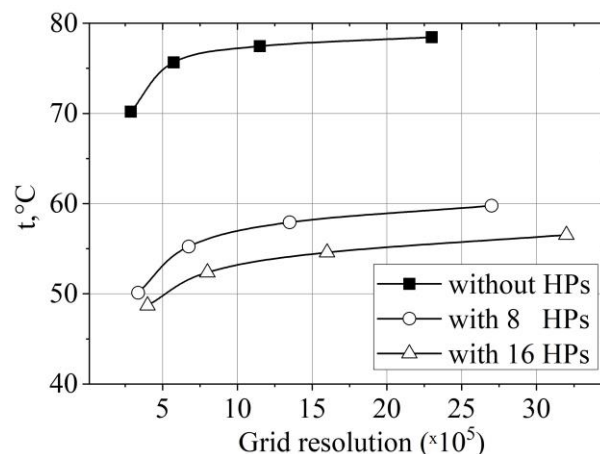


**Fig. 5** Dependence of temperature  $t$  ( $^{\circ}\text{C}$ ) of the hottest transistor (T3) on grid resolution for air speed of 1 m/s in the in the cooling channels of the heat sink housing.

## 4. RESULTS AND DISCUSSION

### 4.1 Temperature distribution across the mounting surface of the heat sink

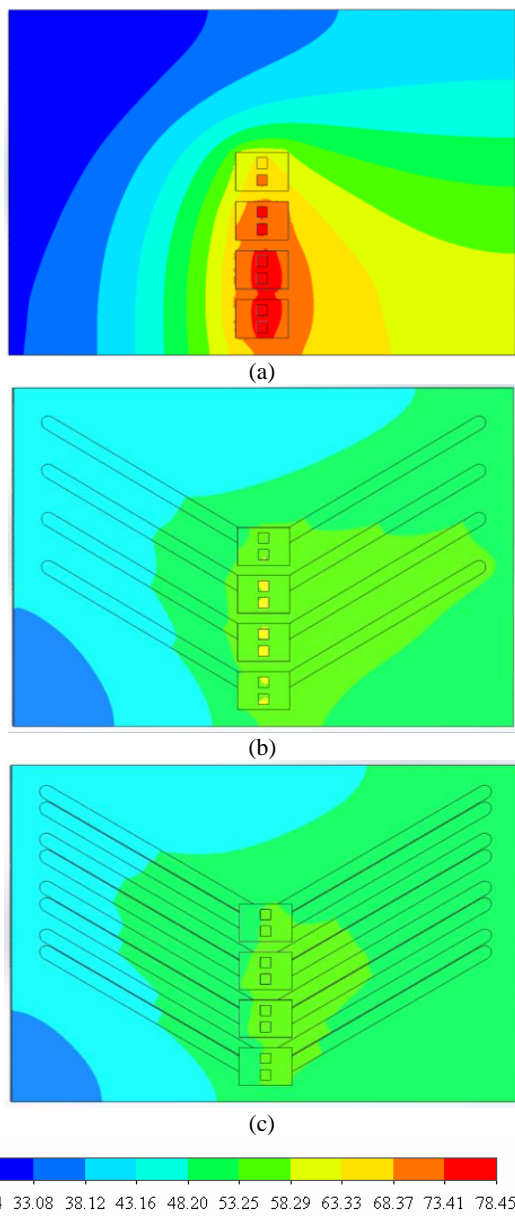
The simulation results on heat-transfer in the cooling system presented in Fig. 6 show the temperature distribution  $t$  across the mounting surface of the cooling system at a constant heat load of 224 W. To provide a clearer comparison of the temperature distribution across the mounting surface of the heat sink housing in three different design options of the cooling system, one figure shows the results for all three designs: with no HPs (Fig. 6, a), with two HPs for each copper mounting plate (Fig. 6, b), and with four HPs for each mounting plate (Fig. 6, c).

Fig. 6 shows the distribution of temperature across the mounting surface of the heat sink housing, as an example, at the same air velocity of 1 m/s in the cooling channels. In these images, the areas of the surface with the same temperature have a certain color, with isotherms indicating

the correspondence of color to a particular temperature range. The images show that the presence of heat pipes, as well as their number, significantly affects the temperature distribution.

Analysis of the temperature fields shown in Fig. 6 reveals the following general patterns:

- the hottest areas on the mounting surface of the heat sink housing are those around the mounting spots of heat-generating microwave elements;
- adding HPs to the design of the heat sink housing significantly changes the temperature distribution over the mounting surface: the surface heating uniformity increases, the absolute values of the temperature of the heat-generating elements decreases;
- doubling the number of HPs, from 8 to 16 units, improves thermal performance only slightly.



**Fig. 6** Temperature field of the heat sink housing without HPs (a), with two HPs (b) and with four HPs (c) for each copper mounting plate at an air velocity of 1 m/s in the cooling channels.

Table 4 shows the absolute values of the main thermal characteristics of the temperature field on the mounting surface of the heat sink housing. Table 4 demonstrates that adding 8 HPs with an

effective thermal conductivity of 5000 W/(m·°C) to the design of the heat sink housing (2 HP for each copper mounting plate with heat-generating transistors) allows reducing the maximum temperature on the mounting surface by 18.69°C (from 78.45 to 59.76°C). Adding 8 more HPs causes the temperature of the hottest part of the surface to decrease by only 3.24°C (from 59.76 to 56.52°C). This indicates that adding 8 more HPs is not justified, because it significantly increases the cost of the cooling system at a minimum thermal effect.

**Table 4** The effect of adding HPs to the design of the heat sink housing on its thermal characteristics at a power input of 224 W and an air velocity of 1 m/s in the cooling channels.

Thermal characteristics	Design option of the cooling system for the T/R module heat sink housing		
	No HPs	With 8 HPs	With 16 HPs
Maximum temperature values on the mounting surface, °C	78.45	59.76	56.52
Minimum temperature values on the mounting surface, °C	28.04	32.85	33.85
Thermal nonuniformity across the mounting surface, °C	50.41	26.91	22.67

Adding the first 8 HPs to the cooling system significantly reduces the nonuniformity of the temperature field across the mounting surface: the difference between the maximum and minimum values of surface temperature is reduced by more than half, i.e. from 50.41 to 26.91°C or 23.5°C. At the same time, adding 8 more HPs further reduces the thermal nonuniformity by only 4.24°C (from 26.91 to 22.67°C).

Thus, when the cooling air velocity in the channels of the heat sink housing is low, the design of the housing has a significant impact on the temperature field distribution across the mounting surface. Adding the HPs to the heat sink housing allows smoothing out the temperature field of the T/R module and improving the thermal conditions for the transistors.

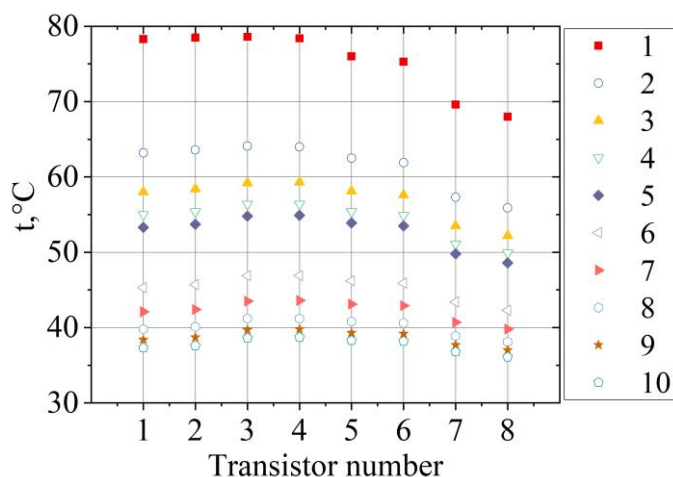
The decrease in the absolute values of the temperature of the transistors and the increase in the uniformity of the surface temperature of the heat sink with heat pipes installed in its base are caused by the physical processes of two-phase heat transfer in the heat pipes via the high-efficiency closed-loop evaporation-condensation cycle. Since the chosen effective thermal conductivity of the heat pipes (5000 W/(m·°C)) is 27.3 times greater than that of the aluminum alloy of the heat sink base (183 W/(m·°C)), the heat from powerful local heat sources (high-power transistors) to remote areas of the heat-transfer surface of the heat sink is transferred by the heat pipes, which have much lower thermal resistance and temperature difference than does the body of the heat sink. Heat flux dispersal from the local heat sources over the heat sink surface via the heat pipes helps to improve the thermal conditions of the transistors and increase the reliability of the T/R module.

The qualitative effect of installing heat pipes into the heat sink base on the leveling of the temperature field over its surface concurs with what is described in the published works of Song *et al.* (2021) Lu *et al.* (2019).

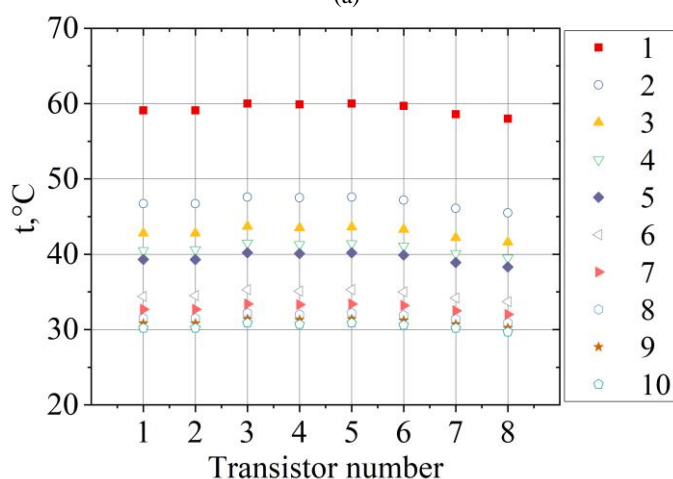
#### 4.2 Influence of cooling air velocity on maximum temperatures of active microwave elements

An important thermal characteristic of the cooling system is the maximum temperature of the active microwave elements, because this parameter affects the reliability of those elements.

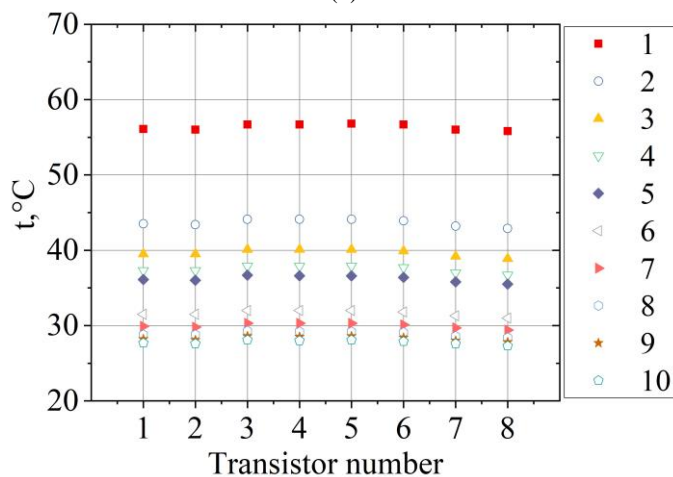
For this reason, the computer simulations results were used to find the maximum temperature values for each transistor.



(a)



(b)



(c)

**Fig. 7** Temperature of the transistors  $t$  (°C) for the heat sink housing without HPs (a), with two HPs (b) and with four HPs (c) for each copper mounting plate at varying air velocity in the cooling channels: 1 – 1 m/s, 2 – 2 m/s, 3 – 3 m/s, 4 – 4 m/s, 5 – 5 m/s, 6 – 10 m/s, 7 – 15 m/s, 8 – 20 m/s, 9 – 25 m/s, 10 – 30 m/s.

The results of determining the temperature of the transistors T1...T8 for the specified velocity of air in the cooling channels are presented in Fig. 7 and in Tables 5-7.

**Table 5** Temperature of the transistors T1...T8 in the heat sink housing without HPs.

Air velocity, m/s	Temperature, °C							
	T1	T2	T3	T4	T5	T6	T7	T8
1	78.3	78.5	<b>78.6</b>	78.4	76.0	75.3	60.6	68.0
2	63.2	63.6	<b>64.1</b>	64.0	62.5	61.9	57.3	55.9
3	58.0	58.4	59.2	<b>59.3</b>	58.1	57.6	53.5	52.2
4	55.0	55.4	<b>56.4</b>	<b>56.4</b>	55.4	54.9	51.1	49.9
5	53.3	53.7	54.8	<b>54.9</b>	53.9	53.5	49.8	48.6
6	51.6	52.0	53.2	<b>53.3</b>	52.2	51.8	48.5	47.3
7	49.7	50.1	51.4	<b>51.5</b>	50.4	50.1	47.0	45.9
8	47.6	48.0	49.2	<b>49.3</b>	48.4	48.1	45.2	44.1
9	46.3	46.7	<b>47.9</b>	<b>47.9</b>	47.2	46.9	44.2	43.1
10	45.3	45.7	<b>46.9</b>	<b>46.9</b>	46.2	45.9	43.4	42.3
15	42.1	42.4	43.5	<b>43.6</b>	43.1	42.9	40.7	39.8
20	39.8	40.1	<b>41.2</b>	<b>41.2</b>	40.8	40.6	38.9	38.1
25	38.4	38.7	39.7	<b>39.8</b>	39.3	39.2	37.7	37.0
30	37.3	37.6	38.6	<b>38.7</b>	38.3	38.2	36.8	36.1

The transistors are numbered from the one closest to the lower edge of the heat sink. The results of thermal simulation of the transistors T1...T8 for the chosen values of cooling air velocity (Fig. 7 and Table 5-7) indicate that, in all design options of the heat sink housing, the highest temperature values are detected in transistors T3 and T4 for all air velocity values. However, in the heat sink housing designs with 8 and 16 HPs, the absolute temperature value of these transistors which is lower than in the heat sink housing with no HPs. For example, at an air velocity of 1 m/s when used in a heat sink housing 8 HP, the temperature of the transistor T3 decreases by 18.6°C, and from 16 HP - by 21.9°C, and the temperature of the transistor T4 decreases by 18.5°C and 21.7°C, respectively.

**Table 6** Temperature of the transistors T1...T8 in the heat sink housing with 8 HPs.

Air velocity, m/s	Temperature, °C							
	T1	T2	T3	T4	T5	T6	T7	T8
1	59.1	59.1	<b>60.0</b>	59.9	60.0	59.7	58.6	58.0
2	46.7	46.7	<b>47.6</b>	47.5	47.6	47.2	46.1	45.5
3	42.8	42.8	<b>43.7</b>	43.5	43.6	43.3	42.2	41.6
4	40.5	40.6	<b>41.5</b>	41.3	41.4	41.1	40.1	39.5
5	39.3	39.3	<b>40.2</b>	40.1	40.2	39.9	38.9	38.3
6	38.1	38.1	<b>39.0</b>	38.9	39.0	38.7	37.8	37.2
7	36.9	37.0	<b>37.9</b>	37.7	37.8	37.5	36.6	36.1
8	35.8	35.8	<b>36.6</b>	36.5	36.6	36.3	35.5	34.9
9	35.0	35.0	<b>35.9</b>	35.7	35.9	35.6	34.8	34.2
10	34.4	34.5	<b>35.3</b>	35.1	35.3	35.0	34.2	33.7
15	32.7	32.7	<b>33.4</b>	33.3	33.4	33.2	32.5	32.0
20	31.5	31.5	<b>32.2</b>	32.0	32.2	31.9	31.4	30.9
25	30.8	30.8	<b>31.4</b>	31.3	31.4	31.2	30.7	30.2
30	30.2	30.2	<b>30.9</b>	30.7	30.9	30.6	30.2	29.7



Using HPs in the heat sink housing design also allowed increasing the thermal uniformity of the transistors, which is particularly important for multi-channel T/R modules (Wang *et al.*, 2016). The greatest increase in the thermal uniformity of the transistors is observed at lower values of the cooling air velocity. Thus, when the air velocity in the cooling channels is 1 m/s, the thermal nonuniformity of the transistors in the heat sink housing without HPs reaches 10.6°C, and this exceeds the allowable value for the temperature difference for the transistors, which is 10°C (Wang *et al.*, 2016). Adding 8 HPs to the heat sink design allowed reducing the thermal nonuniformity of the transistors down to 2°C at a constant cooling air velocity (and to 0.9°C – if the number of HPs was 16).

**Table 7** Temperature of the transistors T1...T8 in the heat sink housing with 16 HPs.

Air velocity, m/s	Temperature, °C							
	T1	T2	T3	T4	T5	T6	T7	T8
1	56.1	56.0	<b>56.7</b>	56.7	56.8	56.7	56.0	55.8
2	43.5	43.4	<b>44.1</b>	44.1	44.1	43.9	43.2	42.9
3	39.5	39.5	<b>40.1</b>	40.1	40.1	39.9	39.2	38.9
4	37.3	37.3	<b>37.9</b>	37.9	37.9	37.7	37.0	36.7
5	36.1	36.0	<b>36.7</b>	36.6	36.6	36.4	35.8	35.5
6	34.9	34.9	<b>35.5</b>	35.5	35.5	35.3	34.7	34.4
7	33.8	33.8	<b>34.4</b>	34.3	34.4	34.2	33.6	33.3
8	32.7	32.7	<b>33.3</b>	33.2	33.2	33.1	32.5	32.2
9	32.0	32.0	<b>32.6</b>	32.5	32.5	32.4	31.8	31.5
10	31.5	31.5	<b>32.0</b>	32.0	32.0	31.8	31.3	31.0
15	29.9	29.8	<b>30.3</b>	30.3	30.3	30.1	29.7	29.4
20	28.8	28.8	<b>29.3</b>	29.2	29.2	29.1	28.6	28.4
25	28.2	28.1	<b>28.6</b>	28.5	28.6	28.4	28.0	27.8
30	27.7	27.6	<b>28.1</b>	28.0	28.1	27.9	27.6	27.3

Thus, an important conclusion follows from the said above – adding HPs to the design of the heat sink housing is an effective and practical way to ensure high thermal uniformity of multichannel T/R module transistors at all chosen values of air velocity in the cooling channels. The sufficient number of HPs is 8, if their effective thermal conductivity is at least 5000 W/(m·°C).

The air velocity in the cooling channels directly affects the efficiency of heat transfer through the surface and the thermal regime of the transistors. The simulation results show (Fig. 8) that when air velocity increases from 1 to 30 m/s, the impact of air velocity on the temperature of the transistors decreases. The most notable effect is achieved in the air velocity range of 1 to 10 m/s. Thus, when velocity increases from 1 to 10 m/s, the temperature of the hottest transistor (T3) decreases by 31.7°C (from 78.6 to 46.9°C) in the heat sink housing without HPs. When the air velocity increases further, from 10 to 30 m/s, the temperature of the transistor decreases by only 8.2°C (from 46.9 to 38.7°C). Adding HPs to the heat sink housing does not change how air velocity affects the temperature of the transistors, but the absolute temperature values do decrease, and this has a positive impact on the reliability of transistors and the T/R module as a whole.

Such nature of the effect of changes in the cooling air velocity on the temperature of the transistors can be explained by the physics of the air movement through the heat sink channels. At low air velocities, a

laminar flow mode is mostly observed. In this case, the thermal boundary layer is quite thick, and the intensity of heat transfer from the heat sink walls to the cooling air is rather weak. Increasing the air velocity reduces the thickness of the boundary layer and increases the heat transfer coefficients, which leads to better temperature conditions for the transistors. Preliminary calculations of the thermal layer thickness for our case showed the following: when the air velocity was increased from 1 to 10 m/s, the layer thickness decreased by about 3 times, while with a further increase in velocity from 10 to 20 m/s, it decreased by about 1.5 times. This indicates that in the velocity range from 1 to 10 m/s, the flow mode is in transition from laminar to turbulent. At the same time, the heat transfer intensity increases, so there is a significant decrease in the temperature of the transistors. At a steady turbulent flow mode, which occurs at the air velocity of about 18-20 m/s, further increase in air velocity does not lead to a significant increase in heat transfer coefficients, so the temperature of transistors decreases more slowly, compared to the laminar and transient flow modes.

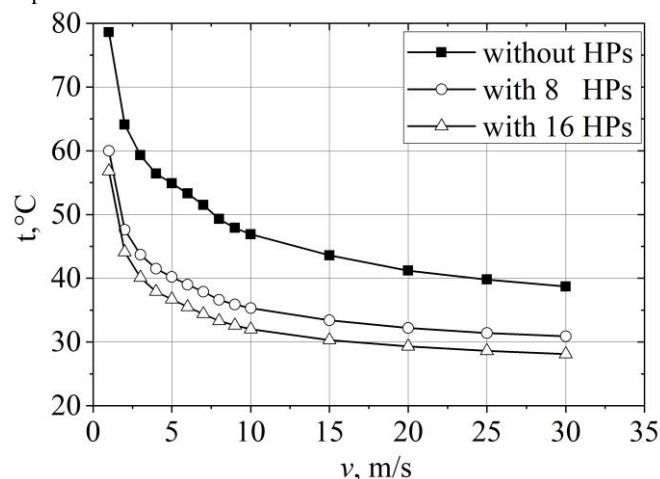


**Fig. 8** Dependence of the temperature  $t$  (°C) of the hottest transistor (T3) on the velocity  $v$  (m/s) of air in the cooling channels of the heat sink housing without HPs (1), with 8 HPs (2), and with 16 HPs (3).

Conclusions about the temperature decrease in the heating zone with an increase in the flow rate of the cooling medium in the heat sink channels, similar to those presented in this article, were published earlier in the works of Zhang *et al.* (2017), Xu *et al.* (2020), Lu *et al.* (2019), Song *et al.* (2021).

Xu *et al.* (2020), Mansouri *et al.* (2018) offered similar data on the reduction of the temperature non-uniformity of heat-generating elements when installing heat pipes into the heat sink base

#### 4.3 Influence of effective thermal conductivity of HPs on maximum temperature values of active microwave elements

The influence of effective thermal conductivity of the HPs on temperature of the active microwave elements (transistors T1...T8) was estimated by comparing the absolute temperature values of the transistors in two heat sink housing designs, one with integrated HPs and another with the HPs replaced by copper rods with a thermal conductivity of 400 W/(m·°C).

The thermal simulation results for the transistors T1...T8 in both heat sink design options for varying effective thermal conductivity are shown in Fig. 9. Effective thermal conductivity varied in a wide range of 1000 to 30,000 W/(m·°C) with an interval of 5000 W/(m·°C). Calculations were performed for the air velocity of 1 m/s in the cooling channels.

Fig. 9a shows that the HPs, unlike the copper rods of the same size, significantly reduce the temperature of the transistors, if the equivalent



thermal conductivity of the HPs is at least 5000 W/(m·°C). At the same time, the thermal uniformity of the transistors also increases. For example, compared to 8 copper rods, 8 HPs with an effective thermal conductivity of 5000 W/(m·°C) reduce the temperature of the hottest transistor (T3) by 17°C (from 79 to 62°C). When using 16 HP instead of 16 copper rods, the temperature of the hottest transistor decreases by almost the same amount (16°C), but with lower absolute values (from 75 to 59°C). Another notable aspect is that the thermal nonuniformity of the transistors is 10°C and 9°C for 8 and 16 copper rods, respectively, and 2.5°C and 1.5°C for 8 and 16 HPs, respectively, which is significantly lower.

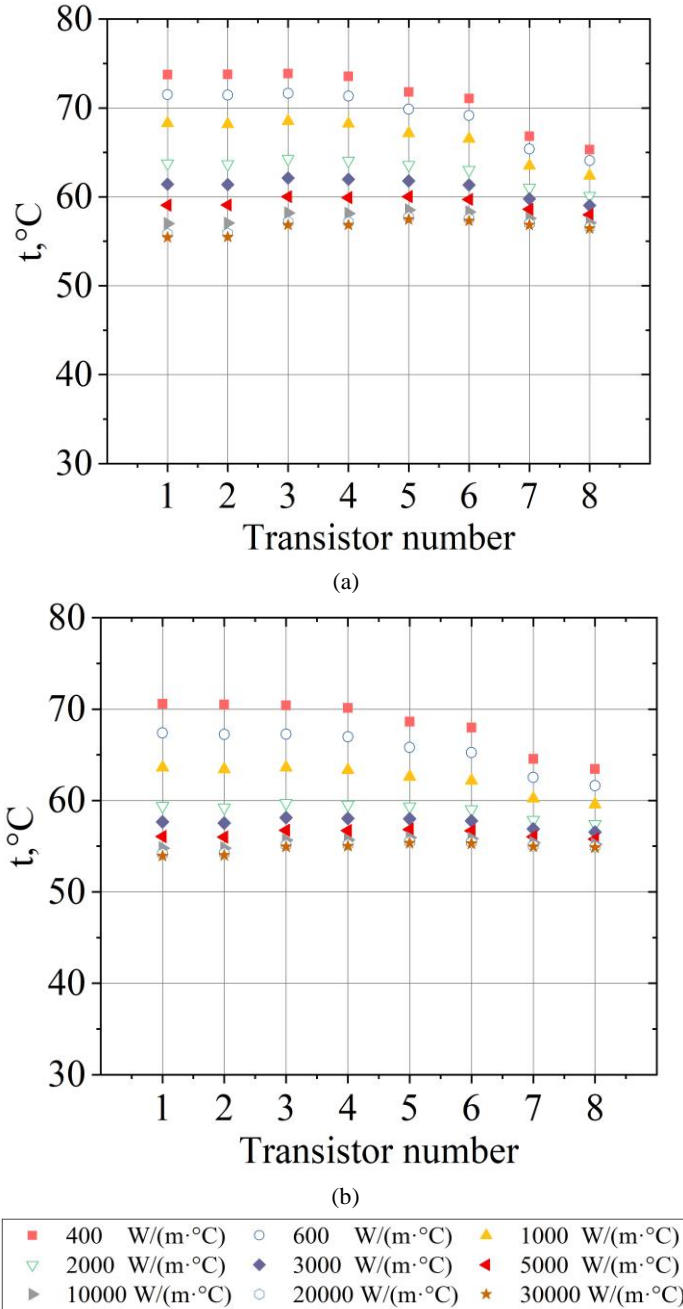


**Fig. 9** Temperature  $t$  (°C) of the transistors T1...T8 at varying effective thermal conductivity of the HPs for heat sink housing design options with 8 HPs (a) and 16 HPs (b).

Since the inexpensive manufacturing technology of flat HPs with a threaded capillary structure allows producing heat pipes with an effective

thermal conductivity range of 5000 to 10,000 W/(m·°C) required for practical use, Fig. 10 shows the simulation results on the dependence of the temperature of the hottest transistor (T3) on the effective thermal conductivity of the heat pipes, obtained with a smaller interval of 1000 W/(m·°C).

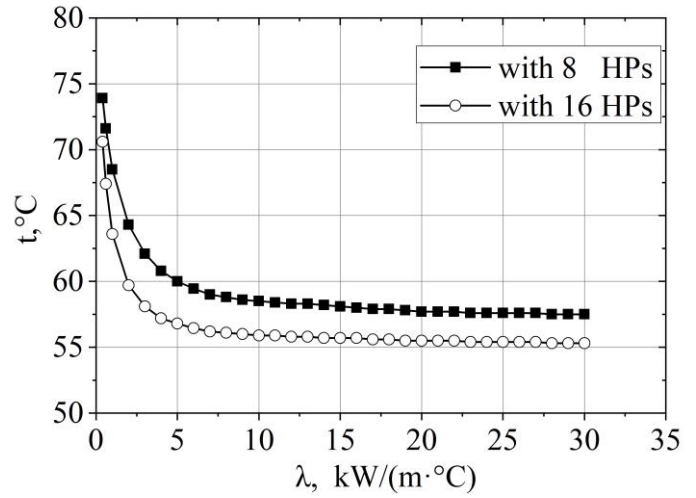


**Fig. 10** Dependence of the temperature  $t$  (°C) of the hottest transistor (T3) on the effective thermal conductivity  $\lambda$  of the HPs at an air velocity of 1 m/s in the cooling channels for the heat sink housing with 8 HPs and 16 HPs.

The effective thermal conductivity  $\lambda$  of heat pipes depends on many factors, the most influential being the thermophysical properties of the working fluid, geometry (the lengths of heat transfer zones and the entire heat pipe, and the diameter of the internal chamber), and heat dissipation. Effective thermal conductivity is directly proportional to heat flux. The increase in the heat flux leads to the transition from the evaporation mode to the boiling mode in the evaporator and causes the changes in the nature of the heat transfer inside the heat pipe. This is primarily due to the activation of the vaporization sites in the heating zone and the increase in their number. At bubble boiling, the effective thermal conductivity  $\lambda$  of the heat pipe increases significantly and the conditions for heat dissipation from the transistors improve. Therefore, the efficiency of heat pipes increases with increasing their effective thermal conductivity to 5000-10,000 W/(m·°C). A further increase in  $\lambda$  has no significant effect on reducing the temperature of the transistors, because it is constrained by the limited external cooling intensity in the heat sink channels.

#### 4.4 Thermal resistance of the cooling system

An important parameter, from a practical standpoint, is the total thermal resistance. The results of computer simulation of the thermal characteristics of the cooling system were used to calculate the total thermal resistance in the range of air velocity of 1 to 30 m/s in the cooling channels. The total thermal resistance  $R$  (°C/W) of the cooling system for the T/R module was determined by the equation:

$$R = \frac{t_{max} - t_{in}}{P},$$

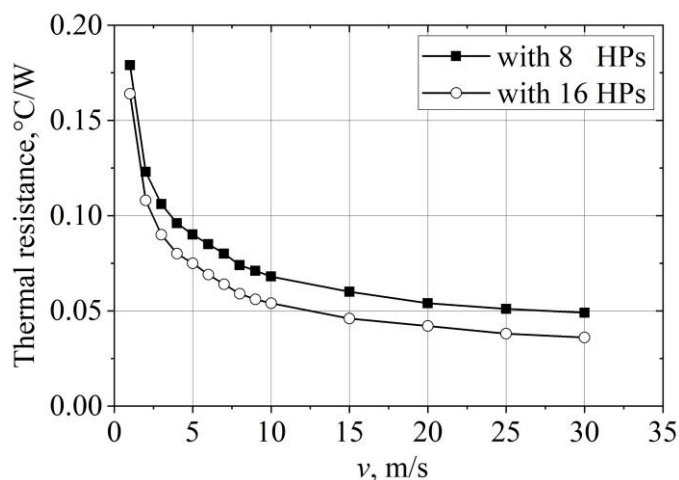
where  $t_{max}$  is the highest temperature of the transistor case, °C;  $t_{in}$  is the cooling air temperature at the inlet to the channels of the heat sink housing, °C;  $P$  is the total power of transistors, W.

Table 8 shows the calculated values of the total thermal resistance of the proposed design options of the cooling system with a heat sink housing with 8 and 16 HPs at an inlet air temperature of 20°C.

**Table 8** Total thermal resistance of the T/R module cooling system for the air velocity of 1 to 30 m/s in the cooling channels.

Air velocity, m/s	Total thermal resistance, °C/W	
	Heat sink with 8 HPs	Heat sink with 16 HPs
1	0.179	0.164
2	0.123	0.108
3	0.106	0.090
4	0.096	0.080
5	0.090	0.075
6	0.085	0.069
7	0.080	0.064
8	0.074	0.059
9	0.071	0.056
10	0.068	0.054
15	0.060	0.046
20	0.054	0.042
25	0.051	0.038
30	0.049	0.036

Fig. 11 shows how the total thermal resistance of the cooling system depends on the air velocity in the channels. The figure indicates that the dependence has a steadily decreasing nature. When the air velocity goes up, the thermal resistance of the cooling system decreases. The reason for this is that increasing air velocity boosts the intensity of heat transfer between the air and the fins of the heat-transfer surface of the heat sink housing. The faster the air moves, the higher the heat transfer coefficient. Thus, the performance of the cooling system increases.



**Fig. 11** Total thermal resistance of the cooling system obtained by computer simulation at different air velocities in the cooling channels for the heat sink housing with 8 HPs and 16 HPs.

The data from Table 8 and Fig. 11 indicate that the total thermal resistance of the new cooling system for the T/R module with flat heat pipes significantly decreases when the air velocity in the cooling

channels is increased from 1 to 10 m/s: from 0.3 to 0.14 °C/W for the design option with 8 HPs and from 0.26 to 0.12 °C/W for the option with 16 HPs. A further increase in air velocity reduces the overall thermal resistance only slightly, but significantly increases the cost of pumping air through the cooling channels.

The trend and the nature of the decrease in the overall thermal resistance with growing cooling flow rate are similar to those described in the paper by Lu *et al.* (2019), Mansouri *et al.* (2018).

## 5. CONCLUSIONS

The performed computer simulation of the thermal characteristics of the new T/R module air cooling system with flat gravity heat pipes with a threaded capillary structure integrated into the heat sink housing allows us to draw the following conclusions.

1. Two proposed design options of the new air cooling system with a heat sink housing based on a cheaper mass-produced heat sink profile for multi-channel APAA T/R modules include 8 and 16 flat gravity heat pipes with a simplified threaded capillary structure. Manufacturing such HPs does not involve power-intensive, high-temperature and lengthy sintering or extrusion processes.

2. Adding such heat pipes to the design of the heat sink housing significantly affects the temperature distribution across the mounting surface of the heat sink housing: the temperature uniformity over the mounting surface increases, while the absolute temperature of the heat generating elements decreases. Thus, for 8 transistors with an input power of 224 W, adding 8 HPs with an effective thermal conductivity of 5000 W/(m·°C) to the design of the heat sink housing has the following effect: the maximum temperature on the mounting surface reduces by 18.69°C (from 78.45 to 59.76°C) and the difference between the maximum and minimum values of the surface temperature reduces more than twice (from 50.41 to 26.91°C).

3. Increasing the number of HPs twofold, from 8 to 16, improves the thermal characteristics of the cooling system only slightly. Therefore, the most rational course of action is integrating 8 heat pipes into the heat sink, two HPs for each copper mounting plate with two transistors.

4. The velocity of the air in the cooling channels directly affects the temperature of the transistors, the effect being most notable when the air velocity is increased from 1 to 10 m/s. Further increase in air velocity from 10 to 30 m/s causes a slower decrease in the temperature of the transistors.

5. It was found that, compared to copper rods of the same size, the heat pipes as part of the heat sink housing design can significantly reduce the temperature of the transistors, while increasing their thermal uniformity, if the equivalent thermal conductivity of the heat pipes is 5000 W/(m·°C) and above. Thus, replacing 8 copper rods with 8 flat HPs with an effective thermal conductivity of 5000 W/(m·°C) reduces the temperature of the hottest transistor by 13.9°C (from 73.9 to 60°C), and the thermal nonuniformity of the transistors reduces from 8.6 to 2.1°C.

6. The total thermal resistance of the new cooling system with flat HPs for T/R modules significantly decreases with increasing air velocity in the cooling channels from 1 to 10 m/s, namely from 0.179 to 0.068 °C/W for the design option with 8 HPs and from 0.164 to 0.054 °C/W for the option with 16 HPs. Further increase in air velocity is impractical, as it reduces the total thermal resistance only slightly, but leads to an increase in the cost of pumping air through the cooling channels.

## ACKNOWLEDGEMENTS

This project was supported by the National Research Foundation of Ukraine under the grant research projects no. 2020.02/0357 and under the project Ministry of Education and Science of Ukraine no. 2407.

## NOMENCLATURE

$P$  power input (W)  
 $R$  thermal resistance ( $^{\circ}\text{C}/\text{W}$ )  
 $t$  temperature ( $^{\circ}\text{C}$ )  
 $v$  air velocity (m/s)

### Greek symbols

$\lambda$  effective thermal conductivity ( $\text{W}/(\text{m}\cdot^{\circ}\text{C})$ )

### Subscripts

in at the inlet  
max maximum value

### Abbreviations

AESA active electronically scanned array  
APAA active phased array antenna  
HP heat pipe  
MMIC microwave monolithic integrated circuits  
T/R transmit/receive

## REFERENCES

- Abdallah, A.S., Yasin N.J., Ameen H.A., 2022, "Thermal performance enhancement of heat pipe heat exchanger in the air-conditioning system by using nanofluid," *Frontiers in Heat and Mass Transfer*, **18**, 10. <https://doi.org/10.5098/hmt.18.10>
- Aslan, J., Puskely, J., Janssen, J.H.J., Geurts, M., Roederer, A., Yarovoy, A., 2018, "Thermal-aware synthesis of 5G base station antenna arrays: An overview and a sparsity-based approach," *IEEE Access*, **6**, 58868 – 58882. <https://doi.org/10.1109/ACCESS.2018.2873977>
- Barbety, S.M., 2011, "Low cost electronically steered phase arrays for weather applications," Doctoral Dissertations Available from Proquest. AAI3445182. <https://scholarworks.umass.edu/dissertations/AAI3445182> (accessed April 13, 2022).
- Beletskiy, V.M., Krivov, G.A., 2005, "Aluminum alloys (composition, properties, technology, application)," *Directory. Ed. Academician I.N. Friedlander*, Komintech, Kiev (in Russian).
- Bhagata, R.D., Deshmukh, S.J., 2021, "Numerical analysis of passive two phase fluid flow in a closed loop pulsating heat pipe," *Frontiers in Heat and Mass Transfer*, **16**, 23. <https://doi.org/10.5098/hmt.16.23>
- Carlson, D., 2017, "Tile Arrays Accelerate the Evolution to Next-Generation Radar," *Microwave Journal*, 1-7. <https://www.microwavejournal.com/articles/27652-tile-arrays-accelerate-the-evolution-to-next-generation-radar> (accessed April 13, 2022).
- Choi, G.W., Kim, H.J., Hwang, W.J., Shin, S.W., Choi, J.J., Jae, S., 2009, "High efficiency class-e tuned doherty amplifier using GaN HEMT," *2009 IEEE MTT-S International Microwave Symposium Digest*, 925-928. <https://doi.org/10.1109/MWSYM.2009.5165849>
- Faghri, A., 2014, "Heat pipes: review, opportunities and challenges," *Front Heat Pipes*, **5**, 1–48. <https://doi.org/10.5098/fhp.5.1>
- Goel, P., Vinoy, K., 2011, "A low-cost phased array antenna integrated with phase shifters cofabricated on the laminate," *Progress In Electromagnetics Research B*, **30**, 255-277. <https://doi.org/10.2528/PIERB11041105>
- Guo, H., Ji, X., Xu J., 2020, "Research and development of loop heat pipe – a review," *Frontiers in Heat and Mass Transfer*, **14**, 14. <https://doi.org/10.5098/hmt.14.14>
- Haupt R.L., and Rahmat-Samii Y., 2015, "Antenna array developments: A perspective on the past, present and future," *IEEE Antennas and Propagation Magazine*, **57**(1), 86-96. <https://doi.org/10.1109/MAP.2015.2397154>
- Herd, J.S., and Conway, M.D., 2016, "The evolution to modern phased array architectures," *Proceedings of the IEEE*, **3**(104), 519-529. <https://doi.org/10.1109/JPROC.2015.2494879>
- Hosseinizadeh, S., Tan F., Moosania, S., 2011, "Experimental and numerical studies on performance of PCM-based heat sink with different configurations of internal fins," *Appl. Therm. Eng.*, **31**(17-18), 3827-3838. <https://doi.org/10.1016/j.applthermaleng.2011.07.031>
- Jarndal, A.H., 2007, "Large-signal modeling of GaN device for high power amplifier design," thesis for acquiring the academic degree of doktor der ingenieurwissenschaften, Kassel University press GmbH. <http://www.uni-kassel.de/upress/online/frei/978-3-89958-258-1.volltext.frei.pdf> (accessed April 13, 2022).
- Kalinchak, V.V., Orlovskaya, S.G., Chernenko, 2012, "Thermal conductivity physics and experimental methods for determining the thermal conductivity of a substance," Odesa: Odesa Mechnikov National University, 52 p. (in Ukrainian). <http://dspace.onu.edu.ua:8080/bitstream/123456789/22393/1/teproprov.pdf> (accessed April 13, 2022).
- Koito, Y., 2019a, "Numerical analyses on heat transfer characteristics of ultra-thin heat pipes: Fundamental studies with a three-dimensional thermal-fluid model," *Applied Thermal Engineering*, **148**, 430-437. <https://doi.org/10.1016/j.applthermaleng.2018.10.119>
- Koito, Y., 2019b, "Numerical analyses on vapor pressure drop in a centered-wick ultra-thin heat pipe," *Frontiers in Heat and Mass Transfer*, **13**, 26. <https://doi.org/10.5098/hmt.13.26>
- Koito, Y., 2021, Numerical analysis of the effect of deviation from a centered wick structure in an ultra-thin flattened heat pipe, *Frontiers in Heat and Mass Transfer*, **16**, 1. <https://doi.org/10.5098/hmt.16.1>
- Kopp, B.A., Billups, A.J., Luesse M.H., 2001, "Thermal Analysis and Considerations for Gallium Nitride Microwave Power Amplifier Packaging," *Microwave Journal*, **44** (12), 72-82.
- Liang, J.-Y.; Lee, Y.-L.; Mao, S.-W.; Tsai, M.-D. 2021, "Design of an integrated heat dissipation mechanism for a quad transmit receive module of array radar," *Appl. Sci.* **11**, 7054. <https://doi.org/10.3390/app11157054>
- Lu, J., Shen, L., Huang, Q., Sun, D., Li, B., Tan, Y., 2019, "Investigation of a rectangular heat pipe radiator with parallel heat flow structure for cooling high-power IGBT modules," *International Journal of Thermal Sciences*, **135**, 83–93. <https://doi.org/10.1016/j.ijthermalsci.2018.09.00>
- Maguire, L., Behnia, M., Morrison, G., 2004, "An experimental and numerical study on heat spreading enhancement in high power amplifier heat sinks," *European Microelectronics and Packaging Symposium*, Czech Republic Prague 16th to 18th June 2004, 1-6. <https://www.researchgate.net/publication/237347849>
- Mansouri, N., Weasner, C., Zaghlool, A., 2018, "Characterization of a heat sink with embedded heat pipe with variable heat dissipating source placement for power electronics applications," *17th IEEE Intersociety Conference on Thermal and Thermomechanical Phenomena in Electronic Systems (ITherm)*, 311-317. <https://doi.org/10.1109/ITHERM.2018.8419599>
- Mochizuki, M., Nguyen, T., Mashiko, K.i, Saito, Yu., Nguyen, T., Wuttijumnong, V., 2011, "A review of heat pipe application including new opportunities," *Front. Heat Pipes*, **2**, 013001. <https://doi.org/10.5098/fhp.v2.1.3001>



Mochizuki, M. and Nguyen, T., 2019, "Review of various thin heat spreader vapor chamber designs, performance, lifetime reliability and application," *Frontiers in Heat and Mass Transfer*, **13**, 12. <https://doi.org/10.5098/hmt.13.12>

Nikolaenko, Yu.E., Baranyuk, A.V., Reva, S.A., Pis'mennyi, E.N., Dubrovka, F.F., Rohachov, V.A., 2019, "Improving air cooling efficiency of transmit/receive modules through using heat pipes," *Thermal Science and Engineering Progress*, **14**, 100418. <https://doi.org/10.1016/j.tsep.2019.100418>

Nikolaenko, Yu.E., Baranyuk, A.V., Reva, S.A., Pis'mennyi, E.N., Dubrovka, F.F., 2020, "Numerical simulation of the thermal and hydraulic characteristics of the liquid heat exchanger of the APAA transmitter-receiver module," *Thermal Science and Engineering Progress*, **17**, 100499. <https://doi.org/10.1016/j.tsep.2020.100499>

Nikolaenko, Yu.E., Pekur, D.V., Sorokin, V.M., Kravets, V.Yu., Melnyk, R.S., Lipnitskiy, L.V., Solomakha A.S., 2021, Experimental study on characteristics of gravity heat pipe with threaded evaporator. *Thermal Science and Engineering Progress*, **26**, 101107. <https://doi.org/10.1016/j.tsep.2021.101107>

Park, J.S., Shin, D.-J., Yim S.-H., Kim, S.-H., 2021, "Evaluate the cooling performance of transmit/receive module cooling system in active electronically scanned array radar," *Electronics* **10**, 1044. <https://doi.org/10.3390/electronics10091044>

Park, T.-Y., Chae, B.-G., Kim, H., Koo, K.-R., Song, S.-C., Oh, H.U., 2021, "New thermal design strategy to achieve an 80-kg-class lightweight X-band active SAR small satellite S-STEP," *Aerospace* **8**, 278. <https://doi.org/10.3390/aerospace8100278>

Parlak M., Yaban M., 2015, "Thermal solution of high flux phased radar antenna for military application," *Proceedings of the ASME 2015 International Technical Conference and Exhibition on Packaging and Integration of Electronic and Photonic Microsystems InterPACK2015. July 6-9, 2015, San Francisco, California, USA*, 1-7. <https://doi.org/10.1115/IPACK2015-48055>

Patent of Ukraine no. 130237, Nikolaenko, Yu.E., Kotov N.N., Gravity heat pipe, Publ. Nov. 26, 2018, Bul. no. 22 (in Ukrainian).

Patent of Ukraine no. 133241, Nikolaenko, Yu.E., Rohachev V.A., A method of manufacturing a gravity heat pipe, Publ. March 25, 2019, Bul. no. 6 (in Ukrainian).

Patent of Ukraine no. 139015, Nikolaenko, Yu.E., Pis'mennyi, E.N., Dubrovka, F.F., Reva, S.A., Baranyuk, A.V., Rohachov, V.A., Kravets V.Yu., Palamarchuk, O.Ya., Housing of the active phased array antennas module, Publ. Dec. 10, 2019, Bul. no. 23 (in Ukrainian).

Patent of Ukraine no. 147733, Nikolaenko, Yu.E., Kravets V.Yu., Kozak D.V., Solomakha A.S., Pekur D.V., Melnyk R.S., Lipnitskiy L.V., Reva S.A., Housing of transmit/receive module for array antenna, Publ. June 09, 2021, Bul. no. 23 (in Ukrainian).

Pengelly, R.S., Wood, S.M., Milligan, J.W., Sheppard, S.T., Pribble, W.L., 2012, "A review of GaN on SiC high electron-mobility power transistors and MMICs," *IEEE Transactions on Microwave Theory and Techniques*, **6** (60), 1764-1783. <https://doi.org/10.1109/TMTT.2012.2187535>

Pekur, D.V., Nikolaenko, Y.E., Sorokin, V.M., 2020a, "Optimization of the cooling system design for a compact high-power LED luminaire," *Semiconductor Physics, Quantum Electronics and Optoelectronics*, **23**(1), 91-101. <https://doi.org/10.15407/spqeo23.01.091>

Pekur, D.V., Sorokin, V.M., Nikolaenko, Yu.E., 2020b, "Thermal characteristics of a compact LED luminaire with a cooling system based

on heat pipes," *Thermal Science and Engineering Progress*, **18**, 100549. <https://doi.org/10.1016/j.tsep.2020.100549>

Pekur, D.V., Sorokin, V.M., Nikolaenko, Yu.E., 2021, "Features of wall-mounted luminaires with different types of light sources," *ELECTRICA*, **21**(1), 32-40. <https://doi.org/10.5152/electrica.2020.20017>

Qian, S., Ge, C., Lou, S., Zhang, Y., Fan, G., Wang, W., 2022, "Experimental and numerical investigations of the transmitting antenna in microwave wireless power transmission with forced air cooling system," *Case Studies in Thermal Engineering*, **33**, 101933. <https://doi.org/10.1016/j.csite.2022.101933>

Rao, J. B. L., Trunk, G. V., Patel, D. P., 1997, "Two low-cost phased arrays," *IEEE Aerospace and Electronic Systems Magazine*, **12** (6), 39-44. <https://doi.org/10.1109/62.587057>

Rathod, S., Sreenivasulu, K., Beenamole, K.S., Ray, K.P., 2018, "Evolutionary trends in transmit/receive module for active phased array radars," *Defence Science Journal*, **68** (6), 553-559. <https://doi.org/10.14429/dsj.68.12628>

Rebeiz, G.M., Paulsen, L.M., 2017, "Advances in low-cost phased arrays using silicon technologies," *2017 IEEE International Symposium on Antennas and Propagation & USNC/URSI National Radio Science Meeting*, 1035-1036. <https://doi.org/10.1109/APUSNCURSINRSM.2017.8072560>

Sarcione M., Puzella A., 2010, "Technology trends for future low cost phased arrays," *IEEE MTT-S Int. Microwave Symp.*, 688-690. <https://doi.org/10.1109/MWSYM.2010.5515448>

Schily, F. and Polifke W., 2021, "Low-order model of the dynamics and start-up of a pulsating heat pipe," *Frontiers in Heat and Mass Transfer*, **17**, 16. <https://doi.org/10.5098/hmt.17.16>

Scott, M., Sampson, MFR, 2003, "Active phased array antenna," *IEEE International Symposium on Phased Array Systems and Technology*, Boston, MA, USA. 119-123. <https://doi.org/10.1109/past.2003.1256967>

Shinohara, N., 2013, "Beam control technologies with a high-efficiency phased array for microwave power transmission in Japan," *Proceedings of the IEEE*, **101**, 1448-1463. <https://doi.org/10.1109/JPROC.2013.2253062>

Singh R., Mochizuki M., Mashiko K., Nguyen T., 2019, "Data center energy conservation by heat pipe based pre-cooler system," *Frontiers in Heat and Mass Transfer*, **13**, 24. <https://doi.org/10.5098/hmt.13.24>

Sobhan C. B., and Peterson G. P., 2019, "Investigations of wire-bonded micro heat pipes - a review," *Frontiers in Heat and Mass Transfer*, **13**, 5. <http://dx.doi.org/10.5098/hmt.13.5>

Song, J.G., Lee, J.H., Park, I.S., 2021, "Enhancement of cooling performance of naval combat management system using heat pipe," *Applied Thermal Engineering*, **188**, 116657. <https://doi.org/10.1016/j.applthermaleng.2021.116657>

Swadish, M.S., Sangram, K.P., 2017, "Thermal design and analysis of an air cooled X-band active phased array antenna," *11th International Radar Symposium India-2017 (IRSI-17)*, NIMHANS Convention Centre, Bangalore INDIA. <http://radarindia.com/Proceedings%20Archive/IRSI-17/004.pdf> (accessed April 13, 2022).

Wang, L., Wang, Z., Wang, C., Li, G., Yin, L., 2016, "Multiobjective optimization method for multichannel microwave components of active phased array antenna," *Mathematical Problems in Engineering*, **2016**, 5398308. <https://doi.org/10.1155/2016/5398308>



Velardo, J., Singh, R., Ahamed, M.S., Mochizuki, M., Date, A., Akbarzadeh, A., 2021, "The thermal management modules using flattened heat pipes and piezoelectric fans for electronic devices," *Frontiers in Heat and Mass Transfer*, **17**, 1.  
<https://doi.org/10.5098/hmt.17.1>

Xu, J., Qian, J., 2020, "Research on heat transfer characteristics of air cooling plate embedded with heat pipes," *Proceedings of the Seventh Asia International Symposium on Mechatronics vol. II, LNEE 589*, 509-517. [https://doi.org/10.1007/978-981-32-9441-7\\_52](https://doi.org/10.1007/978-981-32-9441-7_52)

Zhang, J., Li, R., Xu, X., Wu, C., 2017, "Design of a cooling system for high density integrated phased array antenna test," *Proceedings of the 2017 Sixth Asia-Pacific Conference on Antennas and Propagation Xian, China, 16–19 October (APCAP)*. 1–3.  
<https://doi.org/10.1109/APCAP.2017.8420686>

Zhang, Y.-L., Sun, X., Zeng, F.-K., Yang, J.-B., & Zhou, F.-L., 2021, "Numerical analysis of a prototype pump as turbine at different working conditions," *Frontiers in Heat and Mass Transfer*, **17**(5).  
<https://doi.org/10.5098/hmt.17.5>